

Fig. S1

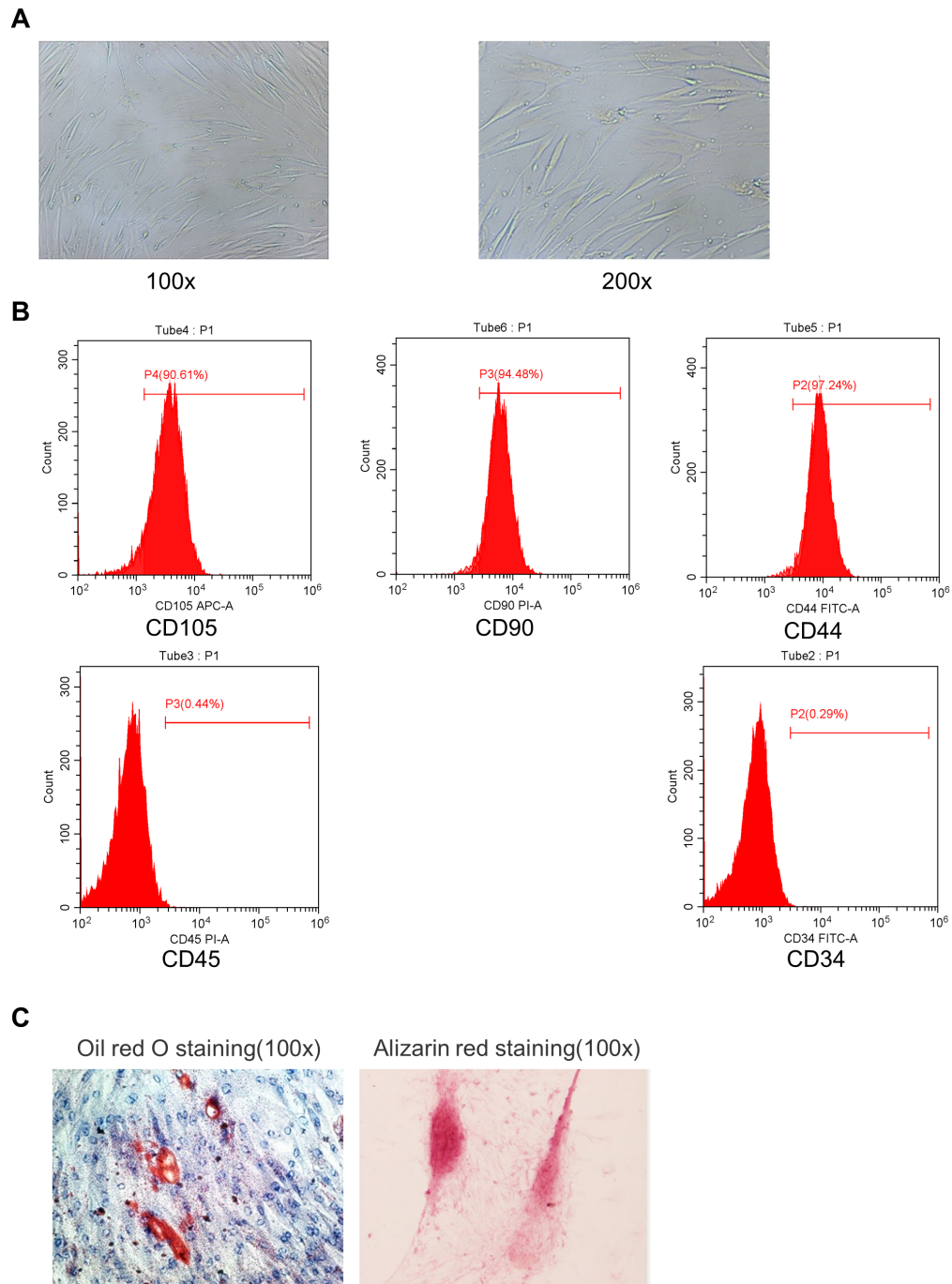


Figure S1. Identification of prepared MenSCs. (A) MenSCs morphology (third generation) were observed by optical microscope. (B) Detection of CD105, CD90, CD44, CD45, CD34 expression in MenSCs by flow cytometry. (C) Oil red O and Alizarin Red staining for detecting the adipogenic osteogenic measurement differentiation abilities of MenSCs.

Fig. S2

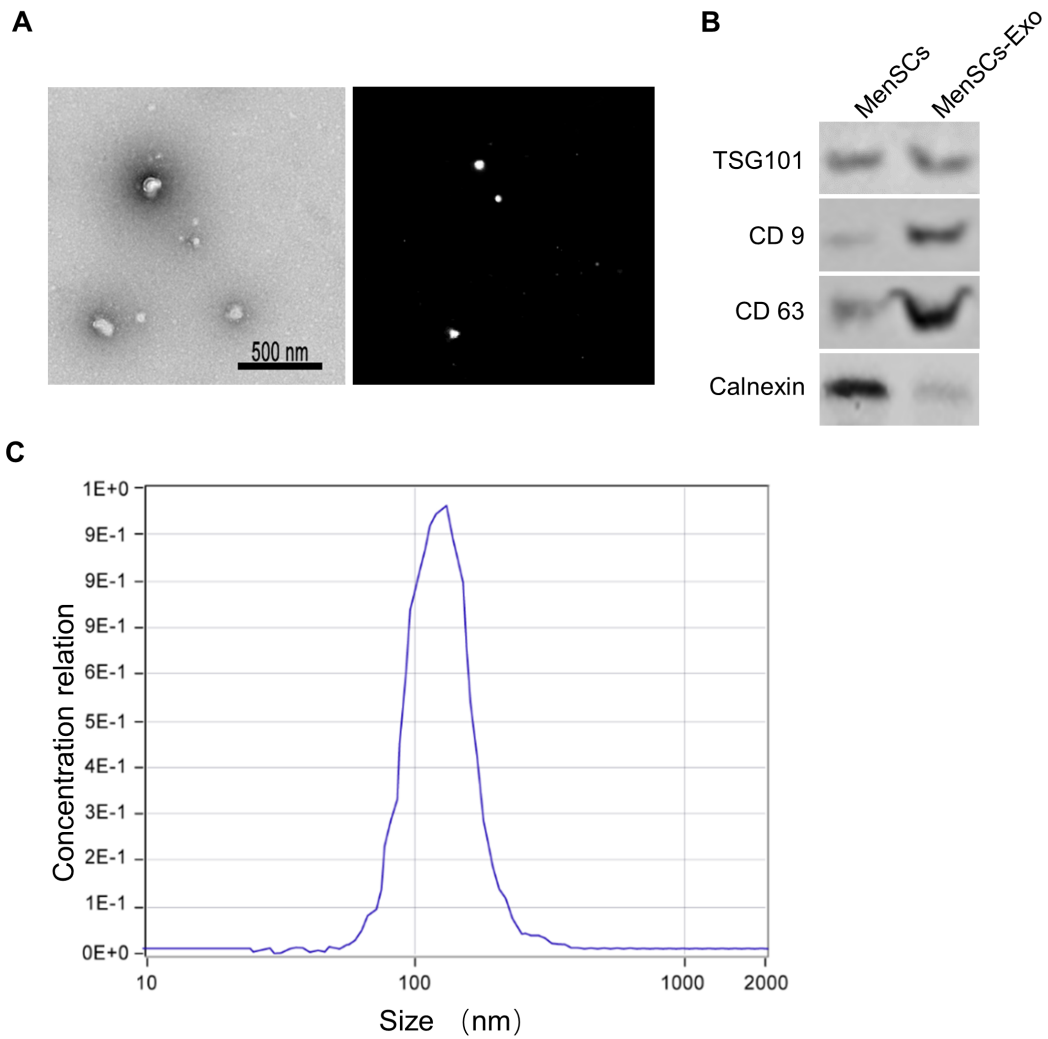


Figure S2. Verification of MenSCs-derived exosome. (A) Electron microscopy results (left) and video screenshots from particle matrix detection (right) of MenSCs-derived exosomes. **(B)** Expression of TSG101, CD9, CD63 and Calnexin were determined by WB in MenSCs-derived exosome. **(C)** Concentration-particle size distribution of exosomes from MenSCs by NTA detection.

Fig. S3

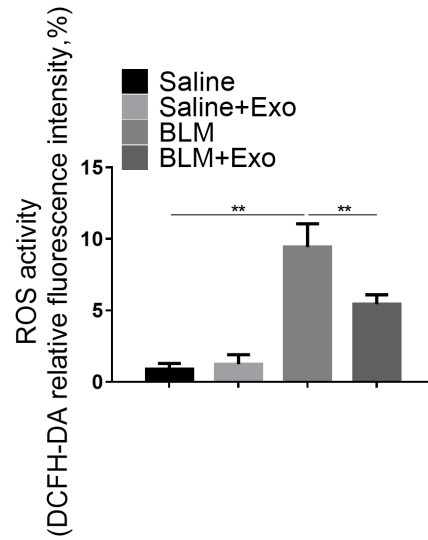


Figure S3. Relative activity of ROS in lung tissue. Quantitative analysis of the ROS level via evaluating the fluorescence intensity. **** $p < 0.01$** .

Fig. S4

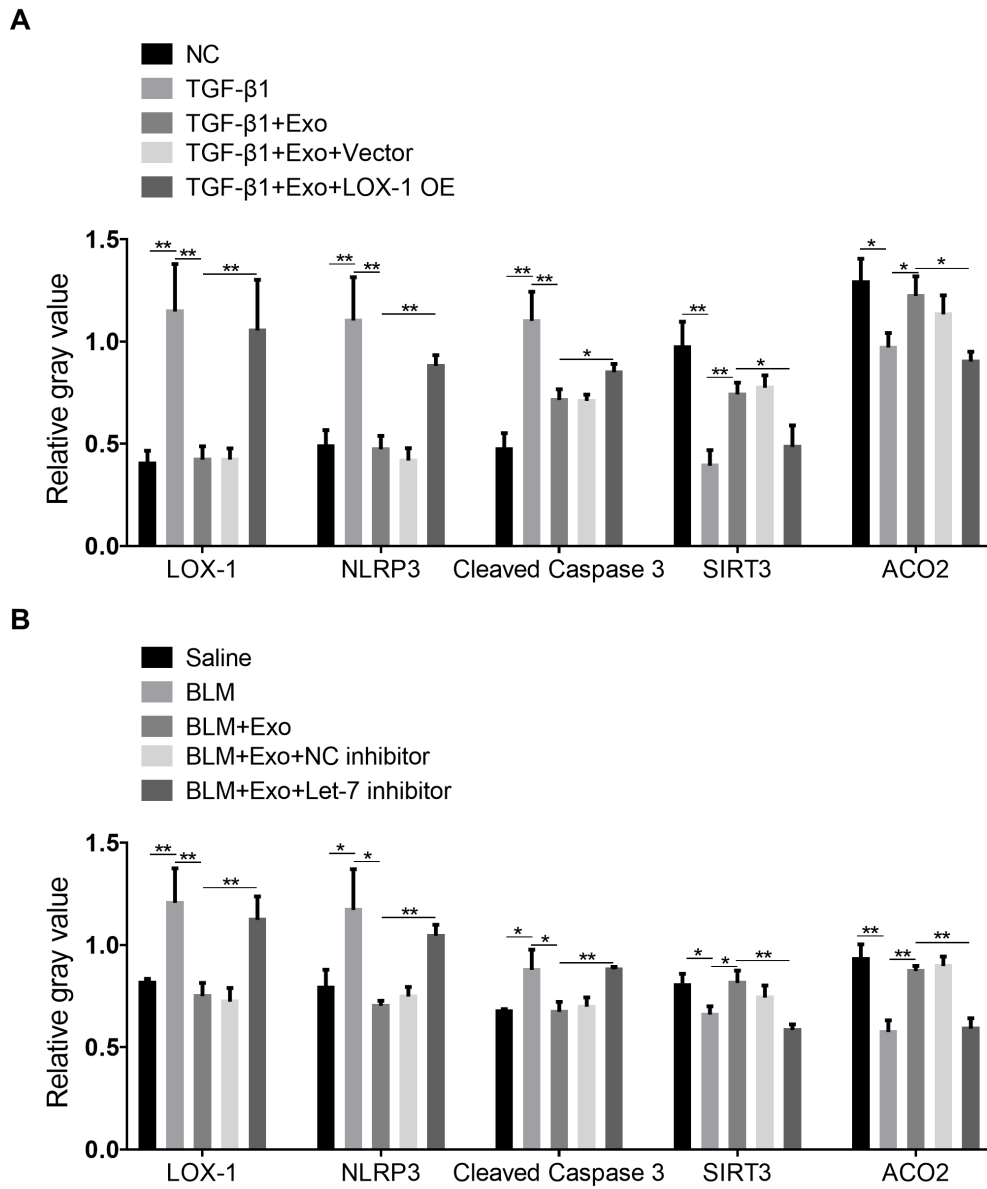


Figure S4. Relative expression of apoptosis- and mtDNA damage-related signal cascades. Quantitative analysis of LOX1/NLRP3/caspase 3 and mtDNA damage markers SIRT3 and ACO2 in MLE-12 cells (A) and in mice lung tissue (B). * $p < 0.05$, ** $p < 0.01$.